

# A novel CCM-TCM multimode control method for totem-pole bridgeless PFC

**Bosheng Sun**

Systems Engineer, Texas Instruments

## Introduction

Power-supply units (PSUs) in data centers must have high efficiency and high power density. The 80 Plus Ruby certification, announced last year, sets the highest efficiency standards for data center PSUs yet. As you can see in **Table 1**, 80 Plus Ruby efficiency is not only higher than 80 Plus Titanium at each load condition, but also requires 90% efficiency at a 5% load, which has never been specified before.

| 80 PLUS Certification    | 230V Internal Redundant |     |     |       |      |
|--------------------------|-------------------------|-----|-----|-------|------|
| Percentage of rated load | 5%                      | 10% | 20% | 50%   | 100% |
| 80 Plus Titanium         |                         | 90% | 94% | 96%   | 91%  |
| 80 Plus Ruby             | 90%                     | 91% | 95% | 96.5% | 92%  |

**Table 1.** 80 Plus certification levels

In the meantime, limited server rack space and increasing power demands have led to high power density. The most recent Modular Hardware System – Common Redundant Power Supply targets 3.6kW power in a 185mm-by-39mm-by-73.5mm form factor which translates to 111W/in<sup>3</sup> power density while other PSU products are still at the 80W/in<sup>3</sup> to 90W/in<sup>3</sup> level.

Server PSU consists of a totem-pole bridgeless power factor correction (PFC) and a DC/DC converter. Traditional control methods used in totem-pole bridgeless PFC are either continuous conduction mode (CCM) or triangular conduction mode (TCM); each method has limitations, however. CCM totem-pole bridgeless PFC can achieve high power density, while its efficiency is limited because of hard switching, especially at light loads where switching losses become dominant. TCM totem-pole bridgeless PFC can achieve excellent

efficiency across the entire load range because of zero voltage switching (ZVS), but requires two or more phases interleaved together to reduce the high inductor current ripple, resulting in low power density and high costs.

**Table 2** compares the two methods.

|      | CCM operation  | TCM operation   |
|------|--|---|
| Pros | <ul style="list-style-type: none"> <li>Low peak-to-peak inductor current ripple</li> <li>Simple control</li> </ul> | <ul style="list-style-type: none"> <li>ZVS</li> </ul>   |
| Cons | <ul style="list-style-type: none"> <li>Hard switching, high switching losses</li> </ul>                            | <ul style="list-style-type: none"> <li>High peak-to-peak inductor current ripple</li> <li>Requires multiphase interleaving to reduce current ripple for high power applications, resulting in low power density and high cost</li> <li>Complex control</li> </ul> |

**Table 2.** Comparing CCM and TCM for totem-pole PFC

To achieve both high efficiency and high power density, totem-pole bridgeless PFC could operate in multimode, as shown in **Figure 1**. At heavy loads or at the peak of an AC half cycle, the desired PFC input current is high and PFC operates in CCM. When the load reduces or at around the AC zero-crossing area where the desired PFC input current is low, PFC switches to TCM and operates with ZVS.

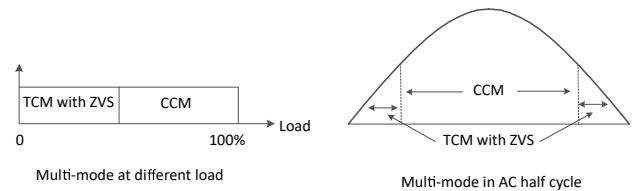


**Figure 1.** CCM\_TCM multimode operation

Compared to pure CCM, multimode control has better efficiency at light loads, attributable to ZVS; compared to pure TCM, there is no need to use multiphase interleaved operation because the inductor current ripple is much lower, significantly reducing both size and system costs. Combining the advantages of both CCM and TCM makes it possible to meet both high-efficiency and high-power-density requirements.

### How to let PFC enter TCM at light loads

TCM operation requires that the inductor current drop to zero at the end of the switching cycle. In CCM PFC, however, the inductor current is almost always greater than zero in the entire AC half cycle because of the high boost inductance. To let the inductor current drop to zero, one way is to choose a boost inductance lower than what CCM PFC uses, but higher than what TCM PFC uses.

Because lower inductance results in higher current ripple, it is important to design the inductor such that the efficiency gained from multimode operation is more than the extra inductor core loss caused by the higher current ripple. The electromagnetic interference filter also needs redesigning, since the inductor current ripple is higher than in CCM.

Another option is to keep the same CCM inductor but use a switching frequency fold-back profile, as shown in **Figure 2**. The switching frequency is the highest (equal to the nominal switching frequency in CCM operation) at the AC peak, and gradually reduces toward AC zero crossing.

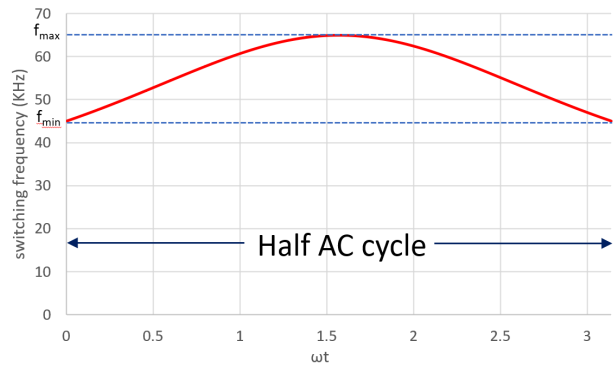


**Figure 2.** Switching frequency profile in an AC half cycle

**Equation 1** calculates the switching frequency across the AC half cycle:

$$f = \frac{1}{\frac{1}{f_{\min}} - \left( \frac{1}{f_{\min}} - \frac{1}{f_{\max}} \right) \sin(\omega t)} \quad (1)$$

where  $f_{\max}$  is the switching frequency as used in traditional CCM operation,  $f_{\min}$  is the minimum switching frequency, and  $\omega t$  is the angular frequency of the AC input voltage.

With the reduced switching frequency, the inductor current will drop to zero at the end of the switching cycle, making TCM control possible. Then the PFC can be controlled to operate in CCM at the AC peak, and switch to TCM with ZVS around the AC zero-crossing area. Further reducing the minimum switching frequency can expand the TCM region but at the cost of reduced loop bandwidth, possibly resulting in poor total harmonic distortion (THD) or even loop instability.

### How to detect zero current

For TCM control, adding a zero current detection (ZCD) circuit by placing a resistor on the PFC ground return path or adding a second winding on the boost inductor will detect the instant that the inductor current drops to zero. Some devices, such as TI's LMG3427R030 gallium nitride (GaN) field-effect transistor (FET), have a built-in ZCD circuit, generating a ZCD signal when the current goes to zero, as shown in **Figure 3**. Using this device as a high-frequency switch can significantly

simplify the design process. The ZCD signal is sent to a microcontroller (MCU) for further processing.

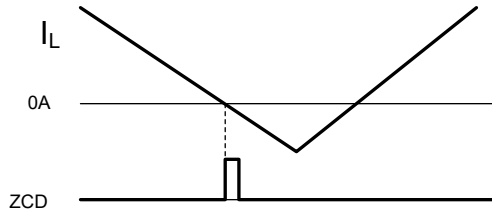


Figure 3. ZCD signal generation

### How to achieve ZVS at TCM

To achieve ZVS operation at TCM, the inductor current needs to go to negative to discharge the switch-node voltage. Upon receiving the ZCD signal, the MCU adds a time delay to this ZCD signal and then uses that delayed ZCD signal to turn off pulse-width modulation (PWM) and reset the PWM counter, as shown in Figure 4. After reset, the next switching period starts and the boost switch turns on. The time delay makes the inductor current go negative because the synchronous switch is still on after the inductor current drops to zero. Appropriately adjusting the delay time will adjust the amount of negative current such that the switch-node voltage will discharge to zero, turning on the boost switch at that moment and achieving ZVS.

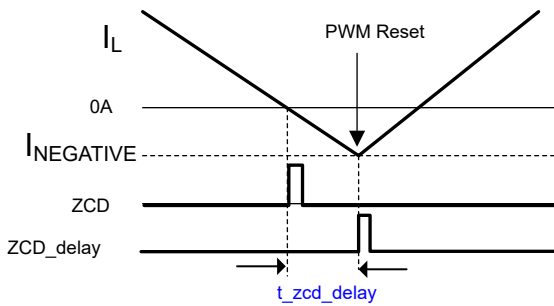


Figure 4. Adding a ZCD delay to reset PWM

For a given dead-time  $\Delta t$  from when the synchronous switch turns off to when the boost switch turns on, Equation 2 calculates the required minimum negative current necessary to fully discharge the switch-node voltage:

$$I_{\text{NEGATIVE}} = -\frac{2 \times C_{\text{OSS}} \times V_{\text{out}}}{\Delta t} \quad (2)$$

where  $C_{\text{OSS}}$  is the output capacitance of the switch and  $V_{\text{out}}$  is the PFC output voltage.

Equation 3 then calculates the required minimum ZCD delay time:

$$t_{\text{zcd\_delay}} = \frac{L \times |I_{\text{NEGATIVE}}|}{V_{\text{out}} - V_{\text{in}}} \quad (3)$$

where  $L$  is the boost inductance and  $V_{\text{in}}$  is the PFC input voltage.

In Equation 3, when  $V_{\text{in}}$  is close to  $V_{\text{out}}$ , the calculated delay time may be too long such that the delayed ZCD signal falls into the next switching period, as shown in Figure 5. Resetting PWM here is wrong. To prevent this, generate an ENABLE window that starts at the beginning of the ZCD signal and ends at the end of the current switching period, as shown in Figure 5. The MCU uses this ENABLE window to AND with the delayed ZCD signal to generate a RESET signal, and then uses that RESET signal to reset PWM. This ensures that the PWM reset can only occur within the same switching cycle.

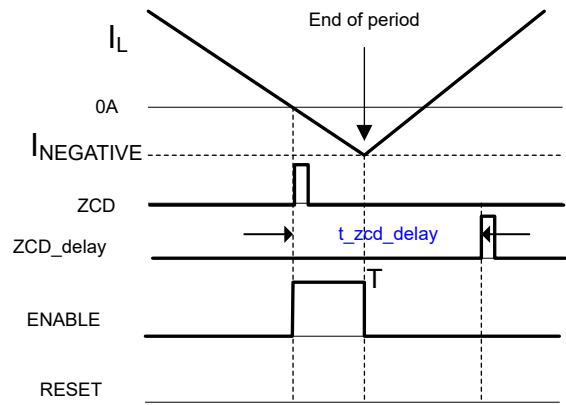
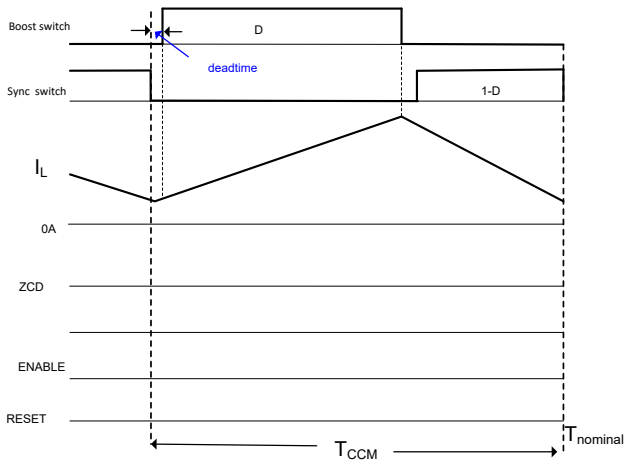


Figure 5. ENABLE window and RESET signal

### Transitioning between CCM and TCM

The transition between CCM and TCM is automatic. At the AC peak or heavy loads, the inductor current is high. It does not drop to zero, and because no ZCD signal is generated, there is no RESET signal. The PWM counter naturally resets at the end of its nominal switching period. And since the switching frequency equals the

nominal switching frequency, PFC operates the same as a traditional CCM PFC, as shown in **Figure 6**.



**Figure 6.** CCM operation at the AC peak

When the AC toward zero crossing, both the inductor current and switching frequency drop, while the inductor current drops to zero before the end of the switching period. The GaN device generates a ZCD signal. Using the time delay calculated by **Equation 3** and ANDing with the ENABLE window – generates a RESET signal. The RESET signal resets the PWM. The synchronous switch turns off before the end of the nominal switching period and the next switching period begins. The actual switching frequency is less than the nominal switching frequency. PFC operates as TCM PFC, as shown in **Figure 7**.

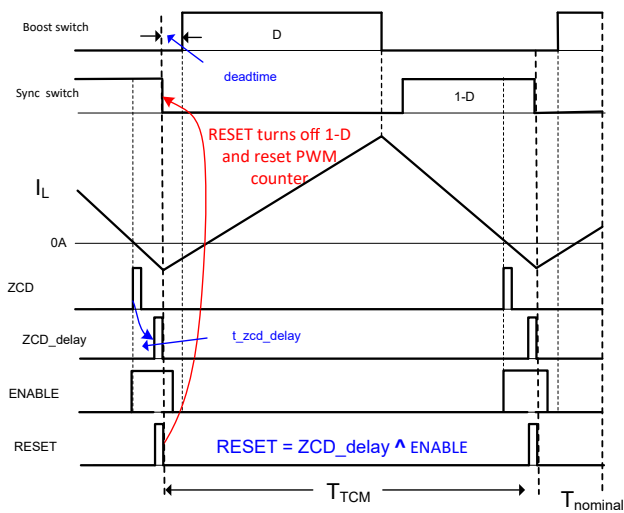


**Figure 7.** TCM operation around AC zero crossing

### Dynamic dead time

In CCM, keeping the dead time to a minimum – the time between when the synchronous switch turns off and the boost switch turns on – will reduce the body-diode conduction time of the boost switch. In TCM, when the synchronous switch turns off, it takes time to discharge or charge the switch-node voltage. Therefore, the dead time needs to be longer. Using a dynamic dead time between CCM and TCM optimizes efficiency.

### Control law and PWM generation

In traditional TCM operation, there is only a voltage loop – no current loop. The boost switch turns on time is determined by a constant  $T_{on}$  control manner. In the multimode control method, the traditional average current-mode controller, as shown in **Figure 8**, generates the PWM duty cycle for both TCM and CCM operations. The controller contains an outer voltage loop ( $G_V$ ) and an inner current loop ( $G_I$ ). The output of  $G_V$  is modulated by the sensed input voltage to be the current command for the current loop. Since the same compensator generates the PWM duty cycle for both CCM and TCM, the mode transition is smooth, with no current distortion during the mode transition.

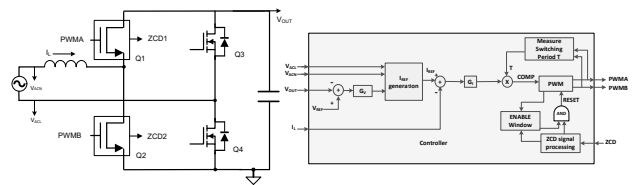


**Figure 8.** Block diagram for proposed CCM\_TCM control

In the MCU, comparing a COMP value to a RAMP signal generates the PWM signal, where COMP is calculated in **Equation 4** by multiplying current loop  $G_i$  output with switching period  $T$ :

$$COMP = G_i \times T \tag{4}$$

In traditional CCM operation, the switching period  $T$  is constant. However, in TCM operation, the RESET signal determines the actual switching period; it is shorter than  $T$ . Using **Equation 4** results in a PWM pulse width longer

than needed, causing  $G_i$  to work harder to compensate. Pushing  $G_i$  to a higher bandwidth can help, but may cause loop instability.

To resolve this issue, let the controller keep measuring the actual switching period. Calculate the COMP value by multiplying the  $G_i$  output with the measured switching period from the previous switching cycle, as shown in Equation 5 and Figure 9. Equation 5 is valid because the PWM period is almost the same in two consecutive cycles.

$$COMP_N = G_i \times T_{N-1} \tag{5}$$

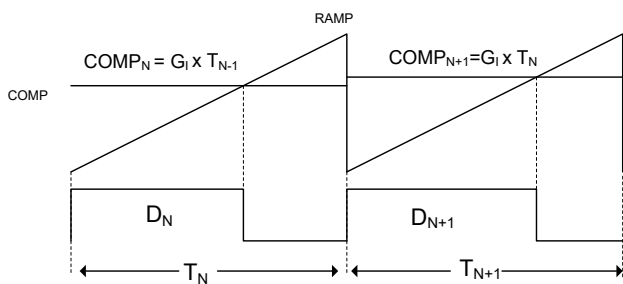


Figure 9. PWM generation

### Test results

This control method was implemented in a 3.6KW totem pole bridgeless PFC [1]. Its maximum switching frequency is 65KHz, the minimum switching frequency is set at 45KHz. The controller uses TI's TMS320F280039C real-time MCU. High-frequency switches use the LMG3427R030 GaN FET, which has a built-in ZCD circuit. A 65KHz interrupt service routine 1 (ISR1) implements the current loop and ZCD delay-time calculation, while a 10KHz interrupt service routine 2 (ISR2) implements the voltage loop. The ZCD delay, ENABLE window, AND logic, and actual switching period measurement are implemented through the TMS320F280039C's configurable logic block (CLB). After configuration, the CLB runs independently without involving the CPU.

The design achieved  $>180W/in^3$  power density and has excellent light-load efficiency. Figure 10 and Figure 11 show the efficiency comparison (tested on the

same board) between this proposed control method and traditional CCM control, with light-load efficiency improving by as much as 2%.

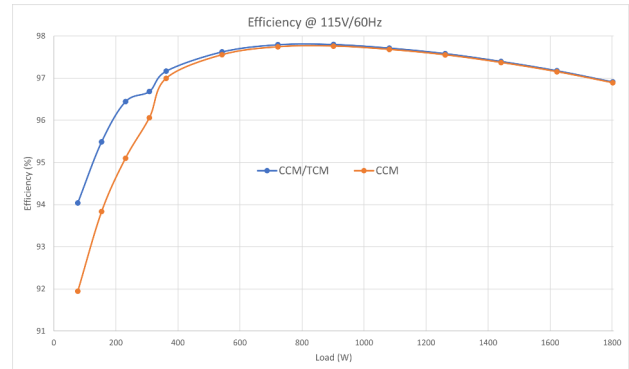


Figure 10. Efficiency comparison at low line

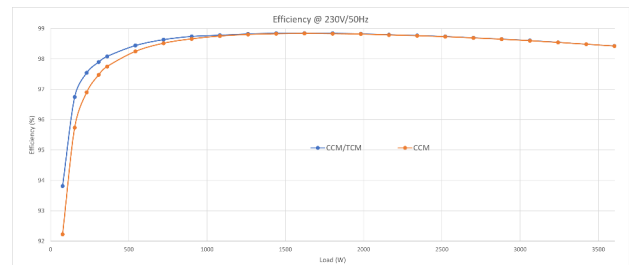


Figure 11. Efficiency comparison at high line

Figure 12 shows the input current waveform at a 50% load, with no current distortion observed during the mode transition.

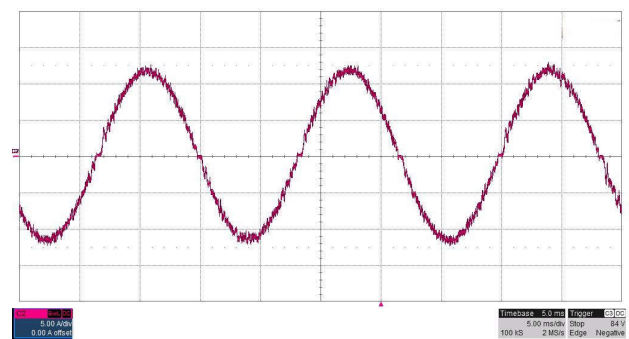


Figure 12. Input current waveform at a 50% load

### Conclusion

Totem-pole bridgeless PFC can achieve both high efficiency and high power density through CCM-TCM multimode operation by letting PFC operate at CCM at heavy loads or at the AC peak, and switching to TCM

with ZVS at light loads or around the AC zero-crossing area. CCM-TCM multimode greatly improves light-load efficiency, with no input current distortion during mode transition. This is very helpful for applications requiring 80 Plus Ruby efficiency.

### References

1. Texas Instruments. n.d. "[3.6kW CCM-TCM Multimode-Controlled Totem-Pole Bridgeless PFC Reference Design](#)." Texas Instruments reference design No. PMP23537. Accessed Feb. 16, 2025.

### About the author

Bosheng Sun is a systems engineer at Texas Instruments, where he focuses on developing digitally controlled, high-performance AC/DC solutions for server and industrial applications. He earned an M.S. in electrical engineering from Cleveland State University in 2003 and a B.S. in electrical engineering from Tsinghua University in Beijing in 1995. He holds six U.S. patents.

**Important Notice:** The products and services of Texas Instruments Incorporated and its subsidiaries described herein are sold subject to TI's standard terms and conditions of sale. Customers are advised to obtain the most current and complete information about TI products and services before placing orders. TI assumes no liability for applications assistance, customer's applications or product designs, software performance, or infringement of patents. The publication of information regarding any other company's products or services does not constitute TI's approval, warranty or endorsement thereof.

All trademarks are the property of their respective owners.

## IMPORTANT NOTICE AND DISCLAIMER

TI PROVIDES TECHNICAL AND RELIABILITY DATA (INCLUDING DATASHEETS), DESIGN RESOURCES (INCLUDING REFERENCE DESIGNS), APPLICATION OR OTHER DESIGN ADVICE, WEB TOOLS, SAFETY INFORMATION, AND OTHER RESOURCES "AS IS" AND WITH ALL FAULTS, AND DISCLAIMS ALL WARRANTIES, EXPRESS AND IMPLIED, INCLUDING WITHOUT LIMITATION ANY IMPLIED WARRANTIES OF MERCHANTABILITY, FITNESS FOR A PARTICULAR PURPOSE OR NON-INFRINGEMENT OF THIRD PARTY INTELLECTUAL PROPERTY RIGHTS.

These resources are intended for skilled developers designing with TI products. You are solely responsible for (1) selecting the appropriate TI products for your application, (2) designing, validating and testing your application, and (3) ensuring your application meets applicable standards, and any other safety, security, regulatory or other requirements.

These resources are subject to change without notice. TI grants you permission to use these resources only for development of an application that uses the TI products described in the resource. Other reproduction and display of these resources is prohibited. No license is granted to any other TI intellectual property right or to any third party intellectual property right. TI disclaims responsibility for, and you fully indemnify TI and its representatives against any claims, damages, costs, losses, and liabilities arising out of your use of these resources.

TI's products are provided subject to [TI's Terms of Sale](#), [TI's General Quality Guidelines](#), or other applicable terms available either on [ti.com](http://ti.com) or provided in conjunction with such TI products. TI's provision of these resources does not expand or otherwise alter TI's applicable warranties or warranty disclaimers for TI products. Unless TI explicitly designates a product as custom or customer-specified, TI products are standard, catalog, general purpose devices.

TI objects to and rejects any additional or different terms you may propose.

Copyright © 2026, Texas Instruments Incorporated

Last updated 10/2025